DELPHI Collaboration

DELPHI 2003-015-CONF-635
12 June, 2003

Measurement of the Open Beauty and Charm Production Cross Sections in $\gamma\gamma$ Collisions using Semileptonic Decays and Double Tagging at $\sqrt{s} = 189$ - 209 GeV

The DELPHI Collaboration
M. Baubillier, C. Carimalo, W. da Silva, F. Kapusta
LPNHE, Paris, France
Ph. Gavillet
CERN, Geneva, Switzerland
M. Chapkine, A. Sokolov
IHEP, Protvino, Russia
V. Pozdniakov
JINR, Dubna, Russia

Abstract

Heavy b and c quark production in $\gamma\gamma$ collisions has been measured through semileptonic decays with the DELPHI detector at LEP. The 413 pb^{-1}of data were collected at centre-of-mass energies from 189 GeV to 209 GeV. The corresponding extracted cross sections $\sigma(e^+e^- \to e^+e^- b\bar{b}X)$ and $\sigma(e^+e^- \to e^+e^- c\bar{c}X)$ are compared to NLO perturbative QCD calculations. The cross section for b production is found to exceed QCD predictions by a factor of about 3. K-lepton double tagging, used for the first time in $\gamma\gamma$ physics, confirms this excess.

Contributed Paper for EPS 2003 (Aachen) and LP 2003 (FNAL)

1 Introduction

Heavy quark production has already been measured in many experiments [1] and an excess of rates, as compared to QCD predictions, has been observed for the production of $b\bar{b}$ pairs. This is indeed a challenging problem for perturbative QCD since it is expected to be fully predictive thanks to the larger quark mass involved [2], and since next-to-leading order corrections do not appear to sufficiently reduce the observed discrepancy that remains at the level of a factor of 2 to 3, at least at HERA or LEP. At LEP, the L3 and OPAL collaborations have already reported on $b\bar{b}$ pair production from $\gamma\gamma$ collisions [1]. We here present a new analysis of this process, performed at the DELPHI detector at LEP. The main mechanisms for heavy quark production in $\gamma\gamma$ collisions are expected to be the direct and the resolved processes depicted in fig. 1 and fig.2, which are of the same order at LEP II energies.

b and c quarks are selected through the muons coming from their semileptonic decays. The distribution of transverse momenta with respect to the closest jet of the muons provides a clean way of tagging.

As a première in two-photon physics, in our analysis we also made use of the K-lepton charge correlation, with kaons being identified with the Ring Imaging Cerenkov (RICH) detector. This allowed to enhance the b signal and to strengthen the observation that the excess really comes from b quark production mechanisms.

2 Data and Monte Carlo samples

The DELPHI detector and its performance have been described in detail elsewhere [3, 4]. Most of the DELPHI subdetectors were used in the analysis here presented : the Time Projection Chamber (TPC), Muon Forward (MUF) and Muon Backward (MUB) for tracking and muon identification, the High density Projection Chamber (HPC), Forward Electromagnetic Calorimeter (FEMC) for electromagnetic energy measurement and the Small angle TIle Calorimeter (STIC) for antitagging condition. Muons with momenta above 2 GeV/c penetrate the Hadron CALorimeter (HCAL) and are recorded in the MUB and MUF.

Data used were collected with the DELPHI detector during the period 1998-2000, with LEP centre-of-mass energies from 189 GeV to 209 GeV. The luminosity sample is about 463 pb^{-1}. The luminosity weighted average e^+e^- center-of-mass energy is approximately $\sqrt{s_{ee}} = 198$ GeV.

PYTHIA6.143 [7] was used as the reference Monte-Carlo generator for describing two-photon events at Leading Order. Light quarks (u,d,s) were generated without mass, using the full default $\gamma^*\gamma^*$ PYTHIA machinery. Masses of heavy quarks (b,c) were taken into account for the direct process only. Dedicated samples for b and c quarks were produced for the direct and the single resolved components according to each year energies and integrated luminosity. The single resolved cross section was taken to be equal to the direct one [17].

Samples of simulated background to antitagged $\gamma\gamma$ processes were used : $e^+e^- \to \tau^+\tau^-$, $e^+e^- \to e^+e^-\tau^+\tau^-$, $e^+e^- \to Z\gamma$, $e^+e^- \to W^+W^-$, $e^+e^- \to ZZ$ and a DIS$e\gamma$ component. All these processes were generated according to BDKRC [8], KORALZ [9], WPHACT [10] and PYTHIA6.159 [7] respectively. The invariant mass distribution of fig.

5 shows the contributions of the various physical processes.

3 Event selection

The strategy for open beauty event selection proceeded in three steps : selection of antitagged two-photon events, muon selection and jet reconstruction.

3.1 Anti-tag events

Charged particles were required to satisfy the following criteria : momentum greater than 0.2 GeV/c, polar angle θ with respect to the beam axis between 10^0 and 170^0, measured track length greater than 30 cm, radial projection of the impact parameter relative to the interaction point smaller than 3 cm, projection of the impact parameter along the beam direction smaller than 7 cm, relative error on the energy measurement smaller than 100 %.

Full calorimetric information was used. The momentum cuts depend upon the detector and were tuned on the Z0 hadronic sample [5]. A neutral particle was accepted if measured by HCAL (momentum greater than 1 GeV/c), HPC (energy greater than 250 MeV) or FEMC (energy greater than 250 MeV).

The events with the particles passing the above criteria were examined as two-photon candidates. The number of charged tracks had to be greater than or equal to 6 (this cut reduces strongly the background coming from τ decay), total energy of charged tracks and neutral below 70 GeV, visible invariant mass greater than 3 GeV/c^2 and lower than 35 GeV/c^2. A track having a transverse momentum with respect to the beam axis greater than 1.2 GeV/c and $|\cos\theta|$ lower than 0.8 was required in order to satisfy the trigger condition requirement [6]. As a result the trigger efficiency is greater than 98 %. Anti-tagging selection required no neutral particle with energy greater than 40 GeV even from the STIC detector at very small angle.

3.2 Muon Identification

Muons with momentum greater than 2 GeV/c were identified by means of the standard muon-tagging algorithm [11] in which the track is extrapolated to each of the layers of the muon chambers, taking into account multiple scattering in the material and the propagation of track reconstruction errors. A fit is then made between the track extrapolation and the position and direction of the hits in the muon chambers. Ambiguities with muon chamber hits associated to more than one extrapolated track are resolved by selecting the track with the best fit. The charged particle is then identified as a muon if the fit is sufficiently good and if hits are found outside the return iron yoke.

In order to remove muons coming from annihilation processes, muon candidates with momentum greater than 20 GeV/c were discarded.

To exclude regions with poor geometrical acceptance, charged particles were accepted if their polar angle θ satisfies either $0.03 < |\cos\theta| < 0.57$ or $0.71 < |\cos\theta| < 0.94$, which defines the barrel region and the forward region, respectively. For isolated muons, the tagging efficiency was found to be 0.82 ± 0.10 [11].

3.3 Jet reconstruction and transverse momentum of muons

The sensitive variable for the beauty events chosen in this analysis is the transverse momentum of the lepton with respect to the direction of the jet to which it belongs, hereafter denoted by p_T. The jet algorithm is defined in the subroutine LUCLUS inside the LUND Monte Carlo program [12], with default parameter D_{join} equal to 2.5 GeV. The jet analysis was performed on charged and neutral particles. The latter should have an energy greater than 800 MeV in order to suppress spurious fluctuations in the jet direction.

The muon candidate was included in the jet finding algorithm, but the lepton momentum was not included in the determination of the jet direction.

The transverse energy of the jet with respect to the beam axis, computed in summing all transverse energy particles in the jet excluding the muon, must be greater than 500 MeV and lower than 8 GeV. The lower cut reduces background from non-perturbative two-photon interactions and the upper cut reduces strongly the background from annihilation processes. After this final cut 651 events remained.

4 Extraction of the b cross section

The p_T-distribution of candidate muons is shown in fig. 6. The corresponding distributions from b and c quark have well separated shapes. The visible b contribution was fitted by minimizing the binned χ^2 :

$$\chi^2 \;=\; \sum (N_\mu - n_\mu)^2/(N_\mu + n_\mu^w) \;\; \text{with} \;\; n_\mu \;=\; \alpha_b n_\mu^b + \alpha_c n_\mu^c + \alpha_{uds} n_\mu^{uds} + n_\mu^{bckgd} \qquad (1)$$

where N_μ is the number of the candidates in a bin and n_μ is the sum of the various contributions in that bin. The quantities n_μ^b, n_μ^c, n_μ^{uds} and n_μ^{bckgd} are respectively the number of expected beauty, charm, light quarks and background events from the Monte-Carlo normalized to the luminosity of the sample. n_μ^w is the variance of the expected events and α_b, α_c, α_{uds} are the corresponding renormalization coefficients.

The coefficient α_c was fixed so as to reproduce the LEP II average total cross section for open charm production $\sigma(e^+e^- \to e^+e^- c\bar{c}X) = 984 \pm 128$ pb [13, 14, 15].

The coefficient α_{uds} was determined selecting hadrons (π, K, p) instead of muons, using the powerful dE/dx particle identification [16]. The uds component is clearly dominant (79 ± 0.7 (stat) %) as shown in fig. 7. α_{uds} is found to be 1.13 ± 0.01(stat). Using another variable such as visible invariant mass gives a similar result.

The α_{uds} fitted value was taken as input to the α_b fit. The result of the fit of (1) gives $N^b_{data} = 118 \pm 26$(stat) events and leads to the corresponding fractions of the various components : $f_b = 18 \pm 1$ (stat) %, $f_c \simeq 41$ %, $f_{uds} \simeq 39\%$ and $f_{bckgd} \simeq 2\%$. The total $b\bar{b}$ event selection efficiency was found to be about 1.7 % . The corresponding χ^2/N_{dof} is 1.3.

The sources of systematics uncertainties are displayed in Table 1. They include : trigger effects, selection cut variables and their discrepancy between data and Monte Carlo on variables on which cuts were applied, as shown in figure 8, muon efficiency and misidentification of 12.5 % [11], the charm cross section error and the jet algorithm uncertainty. Systematic and statistical errors on α_{uds} were estimated using the discrepancy between data and Monte-Carlo selection variables distributions, leading to an error of 4.8 %.

It should be noted that the systematic and statistical errors on α_{uds} rescaling were taken into account but these errors are correlated to muon misidentification.

The error of 3.4 % on the $b \to \mu$ branching ratio was taken from [11]. To account for the uncertainties of the parametrization of the photon partonic density, the fit was done with two values (0.5, 2.) of the ratio of the direct to resolved cross-sections. The corresponding systematic uncertainty was set to half of the fits difference.

All these errors were quadratically summed giving the result

$$\sigma^{e^+e^- \to\ e^+e^- b\bar{b}X} = 14.9\ \pm\ 3.3\ (\text{stat})\ \pm\ 3.4\ (\text{syst})\ \text{pb} \tag{2}$$

5 K-lepton correlations

The charge correlation between the kaon and lepton from the semileptonic decay of heavy quarks is illustrated in fig. 3 and fig. 4. It is a useful tool to increase the purity of b and c events. We have used it to crosscheck the measurement of the b quark production cross-section.

The muon p_T-distribution was fitted as described in Sec. 4. In addition, a kaon had to be identified in the muon jet on the basis of the dE/dx measured in the TPC combined with the Cherenkov radiation detected in the Barrel and Forward RICH [16]. After application of this selection criteria we are left with 171 events in the $K^{\pm}\ell^{\mp}$ sample and 149 in the $K^{\pm}\ell^{\pm}$ one.

To extract the charm cross section from the $K^{\pm}\ell^{\mp}$ sample, we repeated the procedure described in Sec. 4 was applied, except that α_b was fixed to its previously obtained value while α_c was fitted. Muons with transverse momentum p_T lower than 400 MeV were excluded from the fit because data are not well reproduced by the Monte Carlo generator in the low momemtum range, as can be seen from fig. 9. The corresponding fractions of the various components were found to be : $f_{uds} \simeq 35\%$, $f_c \simeq 48\ \%$, $f_b \simeq 16\%$ and $f_{bckgd} \simeq 1\%$. The corresponding χ^2/N_{dof} is 0.37.

Several sources of systematic uncertainties add up to those already discussed in Sec. 4 : kaon selection efficiency, beauty cross section and $b \to c$ branching ratio [11]. All these uncertainties are displayed in table 2.

The measured $c\bar{c}$ cross-section is :

$$\sigma^{e^+e^- \to\ e^+e^- c\bar{c}X} = 937\ \pm\ 191\ (\text{stat})\ \pm\ 206\ (\text{syst})\ \text{pb}. \tag{3}$$

We have then repeated the fit of Sect.4 and found the various components to be : $f_{uds} \simeq 30\%$, $f_c \simeq 38\ \%$, $f_b \simeq 30\%$ and $f_{bckgd} \simeq 2\%$. The corresponding χ^2/N_{dof} is 0.29.

The beauty cross section is then

$$\sigma^{e^+e^- \to\ e^+e^- b\bar{b}X} = 11.4\ \pm\ 4.5\ \text{pb} \tag{4}$$

which is well compatible with result (3).

6 Conclusions

The production cross-section of beauty and charm quarks in two photon collisions at LEP II average center of mass energy of 198 GeV has been measured. The results are

respectively $\sigma^{e^+e^- \to e^+e^- b\bar{b}X} = 14.9 \pm 3.3$ (stat) pb $\pm$ 3.4 (syst) pb and $\sigma^{e^+e^- \to e^+e^- c\bar{c}X} = 937 \pm 191$ (stat) $\pm$ 206 (syst) pb. These values agree with L3 an OPAL measurements. All the published and preliminary results on the total e^+e^- cross-section for b and c production in $\gamma\gamma$ collisions are shown in fig 10. They are compared to the Drees, Krämer, Zunft and Zerwas NLO QCD calculation [17]. For the charm production a significant gluon content in the photon is required. The DELPHI extracted b cross-section is in excess of about 2 standard deviations over the predicted value.

7 Acknowledgements

We wish to thank N. Arteaga for useful discussions. We are greatly indebted to our technical collaborators an to the funding agencies for their support in building and operating the DELPHI detector, and to the members of the CERN SL Division for the excellent performance of the LEP collider.

References

[1] M. Acciari et al. (L3 Collab.), Phys. Lett. **B 453** (1999) 83.
M. Acciari et al. (L3 Collab.), Phys. Lett. **B 467** (1999) 137.
A. Bohrer and O. Krasel (ALEPH Collab.) ALEPH-2000-031.
A. Csilling (OPAL Collab.), hep-ex/0010060.
M. Acciari et al. (L3 Collab.), Phys. Lett. **B 514** (2001) 19.
M. Acciari et al. (L3 Collab.), Phys. Lett. **B 503** (2001) 10.
P. Achard et al. (L3 Collab.), Phys. Lett. **B 535** (2002) 59.

[2] S. Frixione et al., J. Phys. **G 26** (2000) 723

[3] P. Aarnio et al. (DELPHI Collab.), Nucl. Inst. Meth. **A303** (1991) 233.

[4] P. Abreu et al. (DELPHI Collab.), Nucl. Inst. Meth. **A378** (1996) 57.

[5] P. Abreu et al. (DELPHI Collab.) Eur. Phys. J. **C6**(1999) 19

[6] V. Canale et al.,"The DELPHI Trigger System at LEP200", DELPHI/99-7 DAS 188 (22 february 1999).

[7] T. Sjöstrand, Comp. Phys. Comm. **82**(1994) 74.
C. Friberg and T. Sjöstrand, Eur. Phys. J. **C13**(2000) 151 (hep-ph/9907245).

[8] F.A Berends, P.H. Daverveldt, R. Kleiss, Comp. Phys. Comm 4086271, Comp. Phys. Comm 4086285, Comp. Phys. Comm 40863009.

[9] S. Jadach and Z. Was, Comp. Phys. Comm 7994503.

[10] E.Accomando, A. Ballestrero and E. Maina, hep-ex/0204052.

[11] P. Abreu et al. (DELPHI Collab.) Eur. Phys. J.**C20** (2001) 455.

[12] T. Sjöstrand, Comp. Phys. Comm. **39** 347
T. Sjöstrand, PYTHIA 5.6 and JETSET 7.3, CERN-TH/6488-92.

[13] OPAL Coll., A. Csilling, Proc of PHOTON2000, AIP conf. proceeding, v. 571 (2000) 276.

[14] L3 Coll., S. Saremi, Proc of PHOTON2000, AIP conf. proceeding, v. 571 (2000) 266.

[15] DELPHI Coll., A.A Sokolov, Proc of PHOTON2001, (2001) 109.

[16] M. Battaglia, P.M. Kluit, "Particle identification using the RICH detectors based on the RIBMEAN package", DELPHI/96-133 (September 1996)
W. Adam *et al.* , "Analysis techniques for the DELPHI ring imaging Cherenkov detector", DELPHI/94-112 (June 1994)

[17] M. Drees, M. Krämer, J. Zunft and P.M. Zerwas, Phys. Lett. **B 306** (1993) 371.

b systematics : source of uncertainty	$\Delta\sigma^{bb}$ (%)
Event selection : N_{ch}, p_T^{track},W_{vis}, p_μ,$\cos\theta_\mu$, Data/MC discrepancy	16.5
Muon : efficiency, misidentification	9.8
$\sigma^{c\bar{c}}_{<LEP>}$	8.3
Jet reconstruction	7.8
α_{uds} : stat, Data/MC discrepancy on $N_{ch}, p_T^{hadron}, W_{vis}$	3.5
Br($b \to \mu$)	3.4
Ratio direct/resolved 1:2 to 2:1	3.1
Total	23.0

Table 1: b systematics

c systematics : source of uncertainty	$\Delta\sigma^{c\bar{c}}$ (%)
Event selection	12.5
Kaon: efficiency, fragmentation	11.0
Jet reconstruction	10.9
Ratio direct/resolved	5.6
α_{uds}	4.2
Muon : efficiency,misidentification	4.0
$\sigma_{b\bar{b}}$	3.5
Br($c \to \mu$)	3.2
Total	22.0

Table 2: c systematics

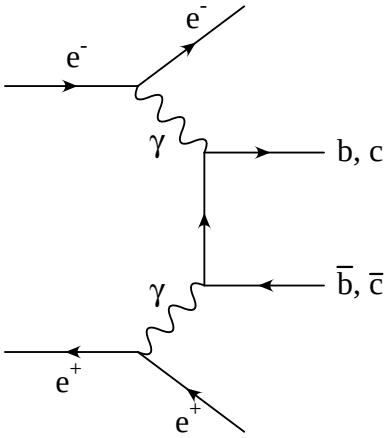

Figure 1: Direct diagram for b and c production

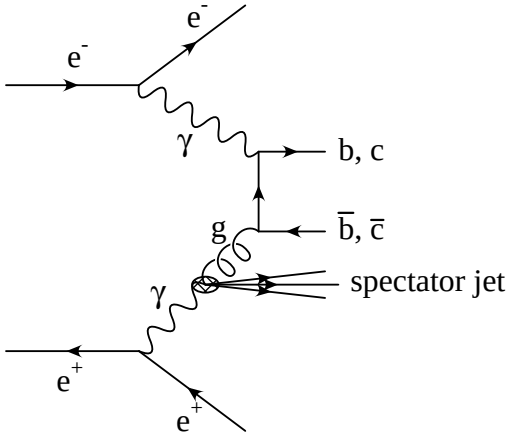

Figure 2: Resolved diagram for b and c production

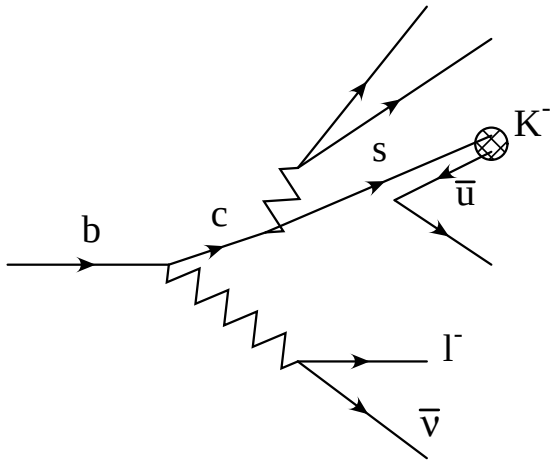

Figure 3: K lepton correlation for b production

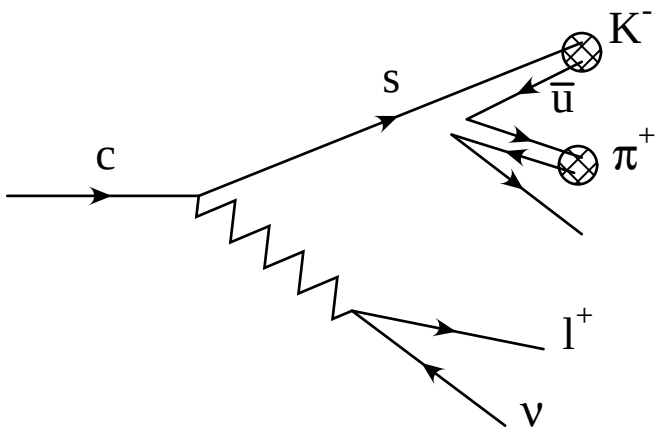

Figure 4: K lepton correlation c production

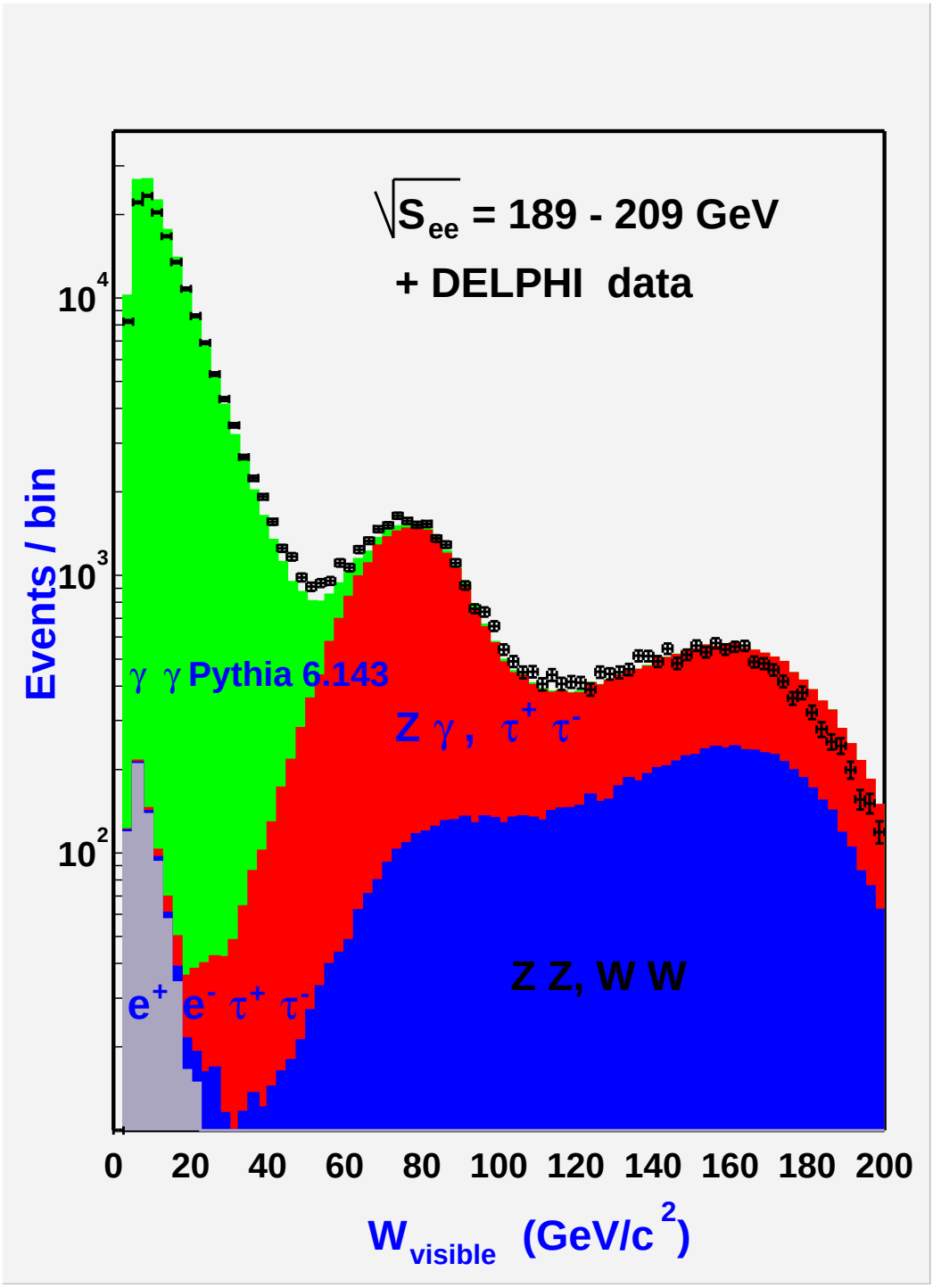

Figure 5: Visible invariant mass distribution for all DELPHI selected data

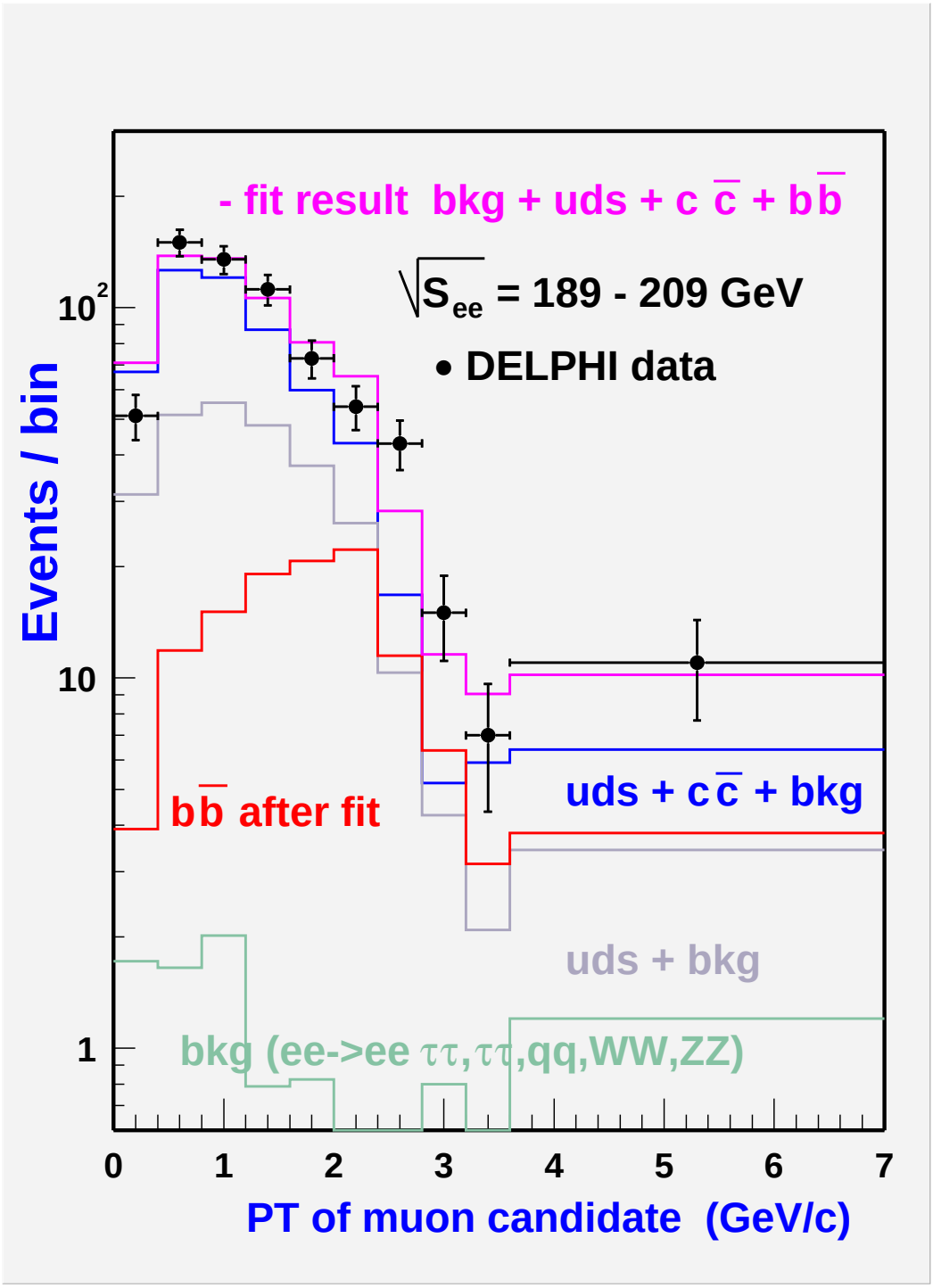

Figure 6: Inclusive muon transverse momentum with all rescaled components

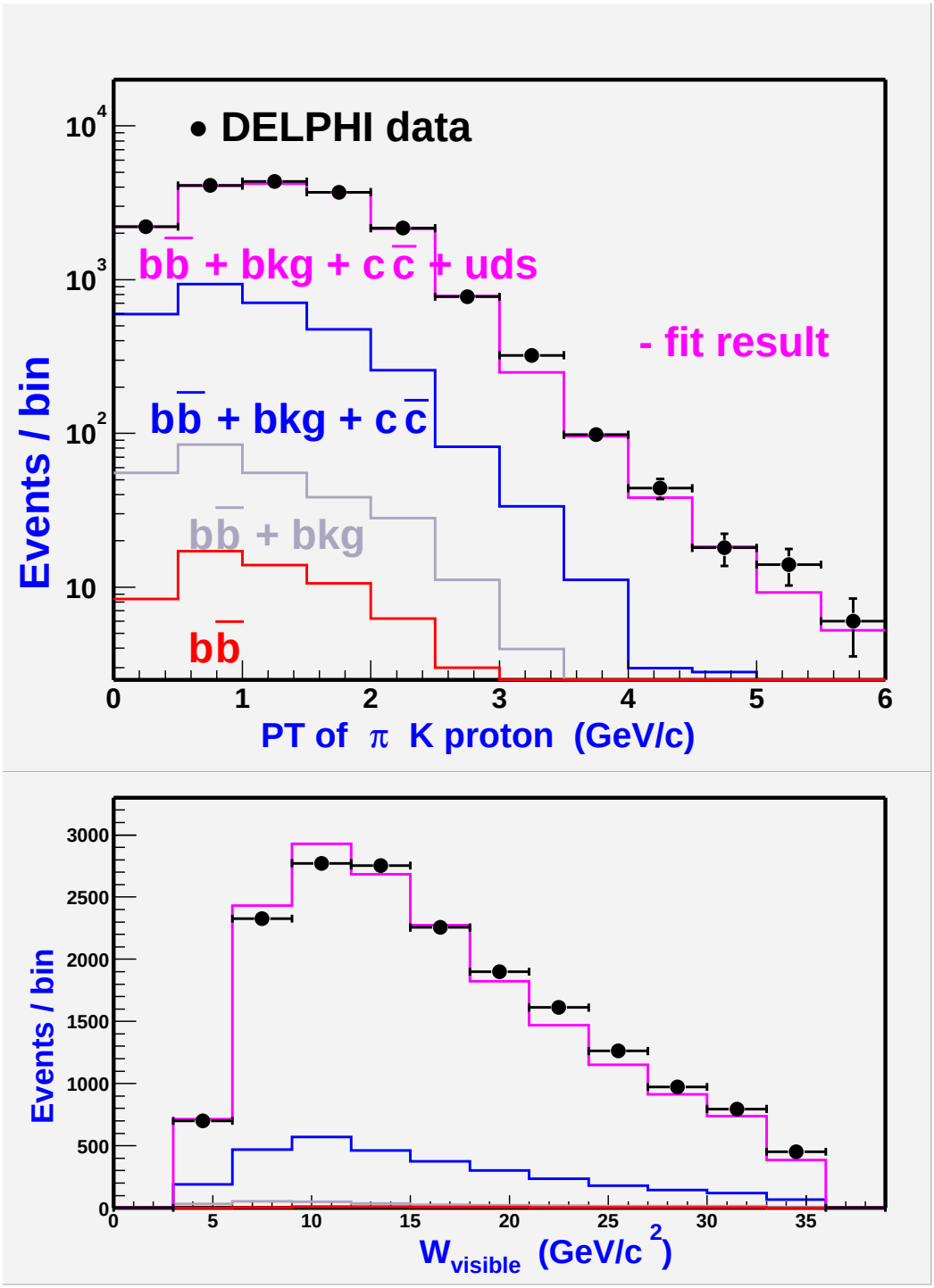

Figure 7: Up : π, K or p inclusive transverse momentum for uds normalization Down : Visible invariant mass for events with at least a π, a K,or a p

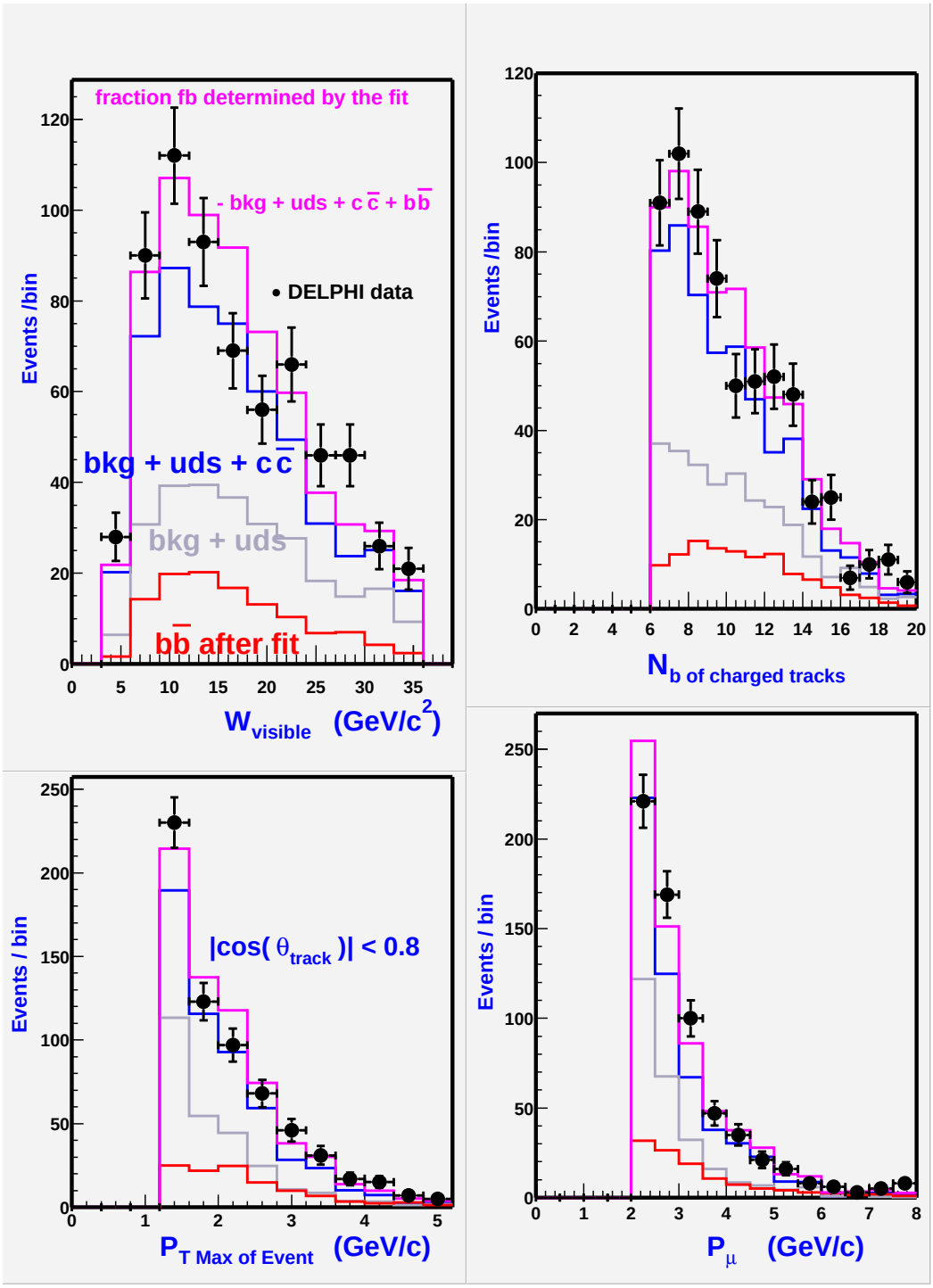

Figure 8: Various distributions after fit

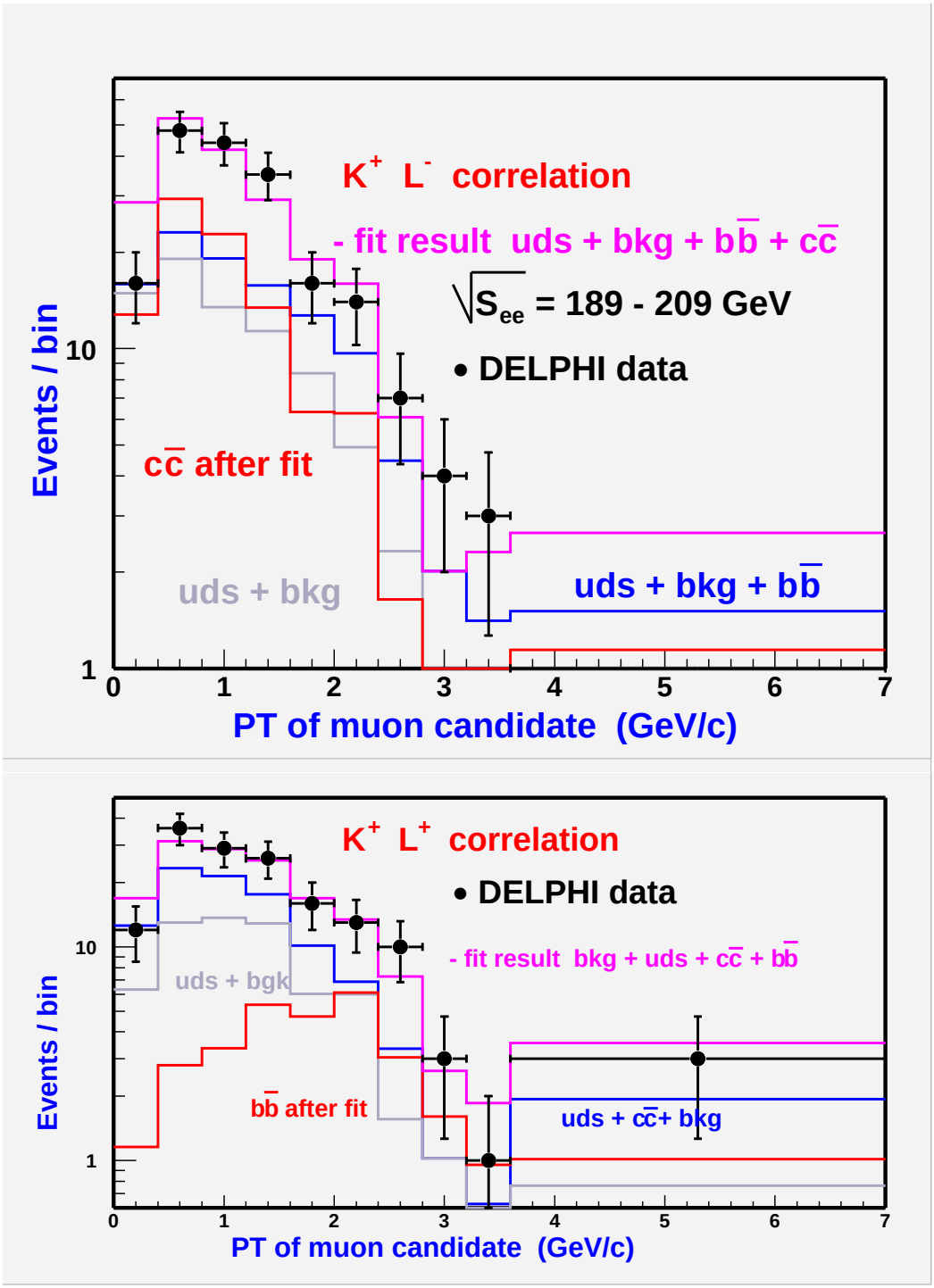

Figure 9: Inclusive muon transverse momentum with K-lepton tagging showing all rescaled components

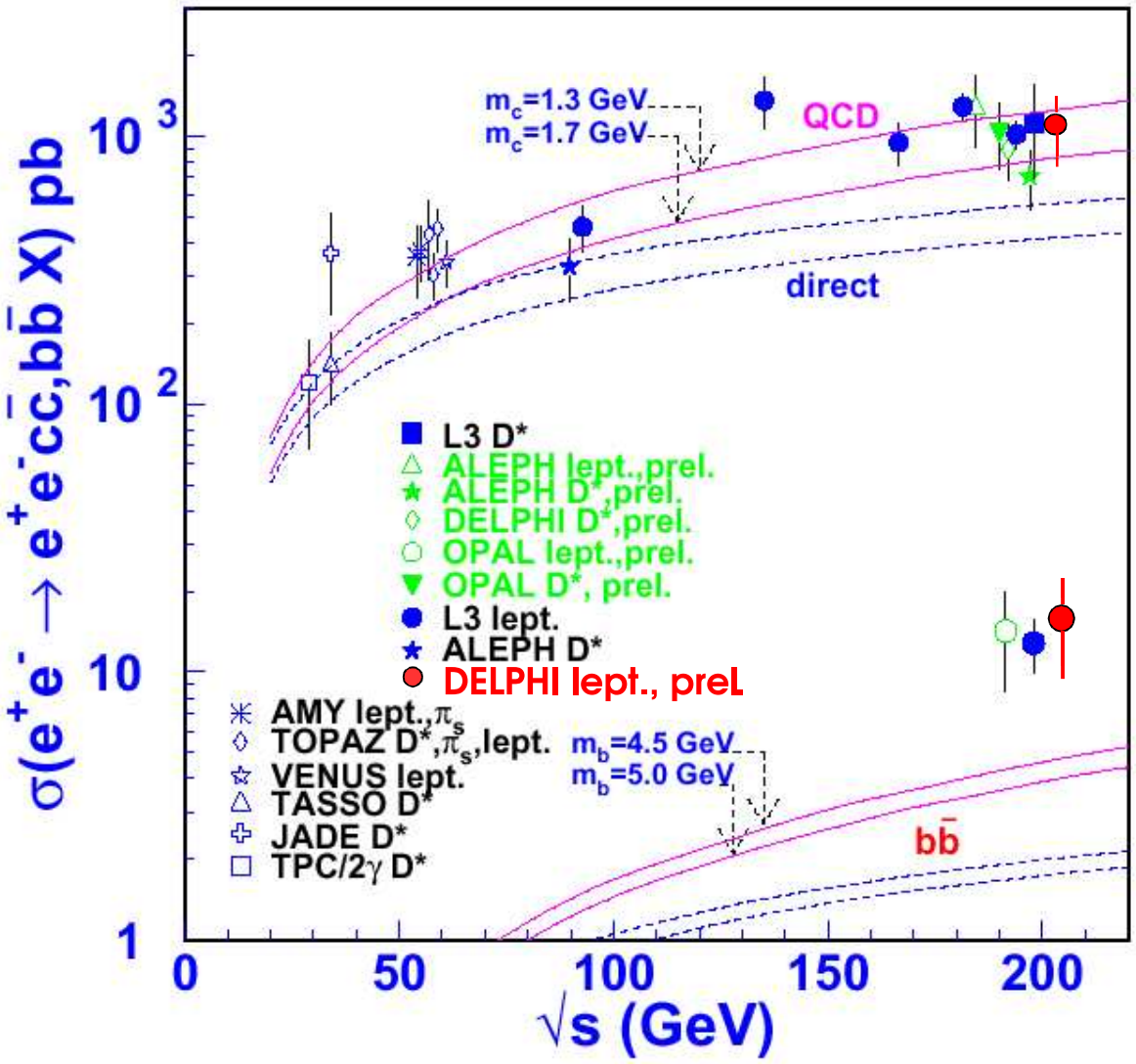

Figure 10: World results